A New Liver-Regeneration Molecular Mechanism Involving Hepatic Stellate Cells, Kupffer Cells, and Glucose-Regulated Protein 78 as a New Hepatotrophic Factor

Journal:	*Journal of Hepato-Biliary-Pancreatic Sciences*
Manuscript ID	JHBPS-2021-0654.R1
Wiley - Manuscript type:	Original Article
Date Submitted by the Author:	24-Mar-2022
Complete List of Authors:	Hagiwara, Kei; Gunma University Graduate School of Medicine School of Medicine, Division of Hepatobiliary and Pancreatic Surgery, Department of General Surgical Science Harimoto, Norifumi; Gunma University, Division of Hepatobiliary and Pancreatic Surgery, Department of General Surgical Science, Yamanaka, Takahiro; Gunma University Graduate School of Medicine, Division of Hepatobiliary and Pancreatic Surgery Ishii, Norihiro; Gunma University Graduate School of Medicine, Division of Hepatobiliary and Pancreatic Surgery Yokobori, Takehiko; Gunma University Graduate School of Medicine School of Medicine, Division of Integrated Oncology Research Tsukagoshi, Mariko; Division of Hepatobiliary and Pancreatic Surgery,, Department of General Surgical Science Watanabe, Akira; Division of Hepatobiliary and Pancreatic Surgery,, Department of General Surgical Science Yoshizumi, Tomoharu; Kyushu University, Department of Surgery and Science Araki, Kenichiro; Gunma University Graduate School of Medicine School of Medicine, Division of Hepatobiliary and Pancreatic Surgery Shirabe, Ken; Division of Hepatobiliary and Pancreatic Surgery,, Department of General Surgical Science;
ORGAN:	LIVER
RESEARCH FIELD:	MOLECULAR BIOLOGY
Keywords: please type five keywords that are identical to those described in the manuscript:	Mac-2-binding protein glycan isomer, hepatic stellate cells, Kupffer cells, glucose-regulated protein 78, liver regeneration
Abstract:	Background /Purpose: To overcome liver failure, we focused on liver-regeneration mechanisms by the activation of hepatic stellate cells (HSCs) and Kupffer cells (KCs). It is known that the HSC-secreted Mac-2-binding protein glycan isomer (M2BPGi) activates KC in the fibrotic liver. However, its importance for liver-regeneration of the HSCs/M2BPGi/KCs axis after hepatectomy is still unknown. This study aims to clarify whether the HSC-derived M2BPGi can activate KCs after

hepatectomy, and elucidate the new molecular mechanism of liver-regeneration.

Methods: We examined the effect of M2BPGi on human hepatocytes and KCs, and explored secretory factors from M2BPGi-activated KCs using proteomics. Furthermore, the effect on liver-regeneration of glucose-regulated protein 78 (GRP78) as one of the M2BPGi-related secreted proteins was examined in vitro and in murine hepatectomy models.

Results: Although M2BPGi had no hepatocyte-promoting effect, M2BPGi promoted the production of GRP78 in KCs. The KC-driven GRP78 promoted hepatocyte proliferation. GRP78 administration facilitated liver regeneration after 70% hepatectomy and increased the survival rate after 90% hepatectomy in mice.

Conclusions: The M2BPGi-activated KCs secrete GRP78, which facilitates liver regeneration and improves the survival in a lethal mice model. Our data suggest that the new hepatotrophic factor GRP78 may be a promising therapeutic tool for lethal liver failure.

1

1 **A New Liver-Regeneration Molecular Mechanism Involving Hepatic Stellate Cells,**

2 **Kupffer Cells, and Glucose-Regulated Protein 78 as a New Hepatotrophic Factor**

3

4 Kei Hagiwara MD[1], Norifumi Harimoto MD, PhD[1], Takahiro Yamanaka MD, PhD[1],

5 Norihiro Ishii MD, PhD[1], Takehiko Yokobori MD, PhD[2], Mariko Tsukagoshi MD,

6 PhD[1,3], Akira Watanabe MD, PhD[1], Kenichiro Araki MD, PhD[1], Tomoharu Yoshizumi

7 MD, PhD[4], and Ken Shirabe MD, PhD[1]

8

9 [1] Division of Hepatobiliary and Pancreatic Surgery, Department of General Surgical

10 Science, Gunma University Graduate School of Medicine, 3-39-22 Showa-machi,

11 Maebashi, Gunma, 371-8511, Japan.

12 [2] Division of Integrated Oncology Research, Gunma University Initiative for Advanced

13 Research (GIAR), 3-39-22 Showa-machi, Maebashi, Gunma, 371-8511, Japan.

14 [3] Department of Innovative Cancer Immunotherapy, Gunma University Graduate

15 School of Medicine, 3-39-22 Showa-machi, Maebashi, Gunma, 371-8511, Japan.

16 [4] Department of Surgery and Science, Graduate School of Medical Sciences, Kyushu

17 University, 3-1-1 Maidashi, Higashiku, Fukuoka, 812-8582, Japan.

18

19

20 **Corresponding Author:** Norifumi Harimoto MD, PhD

21 Division of Hepatobiliary and Pancreatic Surgery, Department of General Surgical

22 Science, Gunma University Graduate School of Medicine, 3-39-22 Showa-machi,

23 Maebashi, Gunma, 371-8511, Japan.

24 Tel: +81-027-220-8224

2

1   Fax: +81-027-220-8230

2   E-mail: nharimotoh1@gmail.com

3

4   **Keywords:** Mac-2-binding protein glycan isomer; hepatic stellate cells; Kupffer cells;

5   glucose-regulated protein 78; liver regeneration.

6

7   **List of word count, table count, and figure count**

8   Abstract: 200

9   Manuscript: 4855

10   Tables: 0

11   Figures: 7

12

1 **Abstract**

2 **Background /Purpose:** To overcome liver failure, we focused on liver-regeneration

3 mechanisms by the activation of hepatic stellate cells (HSCs) and Kupffer cells (KCs).

4 It is known that the HSC-secreted Mac-2-binding protein glycan isomer (M2BPGi)

5 activates KC in the fibrotic liver. However, its importance for liver-regeneration of the

6 HSCs/M2BPGi/KCs axis after hepatectomy is still unknown. This study aims to clarify

7 whether the HSC-derived M2BPGi can activate KCs after hepatectomy, and elucidate

8 the new molecular mechanism of liver-regeneration.

9 **Methods:** We examined the effect of M2BPGi on human hepatocytes and KCs, and

10 explored secretory factors from M2BPGi-activated KCs using proteomics. Furthermore,

11 the effect on liver-regeneration of glucose-regulated protein 78 (GRP78) as one of the

12 M2BPGi-related secreted proteins was examined *in vitro* and in murine hepatectomy

13 models.

14 **Results:** Although M2BPGi had no hepatocyte-promoting effect, M2BPGi promoted

15 the production of GRP78 in KCs. The KC-driven GRP78 promoted hepatocyte

16 proliferation. GRP78 administration facilitated liver regeneration after 70%

17 hepatectomy and increased the survival rate after 90% hepatectomy in mice.

18 **Conclusions:** The M2BPGi-activated KCs secrete GRP78, which facilitates liver

19 regeneration and improves the survival in a lethal mice model. Our data suggest that the

20 new hepatotrophic factor GRP78 may be a promising therapeutic tool for lethal liver

21 failure.

22

23 **Abbreviations**

4

1   CAGE, Cap analysis gene expression; CL, Clodronate liposome; CM, Conditioned

2   media; CT, Computed tomography; DMEM, Dulbecco's modified Eagle medium; FLR,

3   Future liver remnant; HGF, Hepatocyte growth factor; HSC, Hepatic stellate cells; KC,

4   Kupffer cells; LR, Liver remnant; NOS, Nitric oxide synthase; SD, Standard deviation;

5   WB, Western blotting; WFA, *Wisteria fluoribunda* agglutinin

6

1 **Introduction**

2 Complex networks of inflammatory, proliferative, and metabolic signals in hepatocytes

3 are involved in the remarkable regenerative ability of liver after hepatectomy.[1]

4 However, despite the high regeneration ability of the resected liver, unavoidable liver

5 failure and death after hepatectomy remains an important clinical issue.[2]

6 It is known that activation of hepatic stellate cells (HSCs) by the increase in portal vein

7 flow and sinusoidal blood flow velocity plays a key role in the initiation and

8 progression of liver regeneration after hepatectomy.[3, 4] Activated HSCs, which play a

9 central role in hepatic fibrosis progression, promote liver regeneration after

10 hepatectomy by producing a wide array of secretory factors, including cytokines and

11 chemokines.[5] However, it is not fully elucidated what secretory factors contribute to

12 liver regeneration by activated HSCs. Mac-2-binding protein glycan isomer (M2BPGi)

13 has been reported to be one of the secretory factors derived from activated HSCs.[6]

14 M2BPGi has terminal N-acetylgalactosamine motifs with carbohydrate structures that

15 bind to *Wisteria fluoribunda* agglutinin (WFA) lectin.[7] Activated-HSC-derived

16 M2BPGi have already been approved as a noninvasive liver fibrosis marker.[8, 9] The

17 concentration of blood M2BPGi was reported to be elevated in patients with various

18 chronic inflammatory diseases with liver fibrosis such as hepatitis B, hepatitis C

19 alcoholic hepatitis, and nonalcoholic steatohepatitis.[6, 10] Interestingly, the

20 concentration of M2BPGi decreases rapidly after treatment of hepatitis C regardless of

21 the degree of fibrosis. Therefore, it was suggested that M2BPGi might reflect not the

22 liver fibrosis but the activation of HSCs.[6] The M2BPGi secreted by HSCs activates

23 Kupffer cells (KCs), which have been known to play an important role in liver

24 regeneration.[9, 11] However, there is still inadequate knowledge regarding how the

1   HSCs activate KCs and how the activated KCs facilitate liver regeneration after

2   hepatectomy.

3   This study aims to clarify whether the HSC-derived M2BPGi can activate KCs in the

4   damaged liver by fibrosis and liver failure after hepatectomy, and elucidate how the

5   activated KCs after hepatectomy can promote hepatocyte proliferation and liver

6   regeneration.

7

8   **Methods**

9   ***Clinical samples and cell lines***

10   All 24 serum samples were derived from the donor patients of living donor liver

11   transplant three days after the operation (10 right lobectomies, 13 left lobectomies, and

12   one posterior segmentectomy) in Kyushu University Hospital. We received approval for

13   this research from the ethics committee of Kyushu University and Gunma University

14   (HS2019-033). The postoperative liver-regeneration rate of the patients was calculated

15   by the following formula: all liver volumes are measured using computed tomography

16   (CT); total liver volumes and future liver remnant (FLR) volumes were measured from

17   a CT scan of the liver before operation; the liver remnant (LR) volumes were measured

18   from the postoperative day (POD) 7; the total and segmental early regeneration indexes

19   were defined as ($[V_{LR} - V_{FLR}]/V_{FLR}$) × 100, where V_{LR} is the volume of the LR and V_{FLR}

20   is the volume of the FLR.[12] The expected resected liver volumes were also measured

21   from a CT scan of the liver before operation.

22   PXB cells (human hepatocytes) were purchased from Phoenix Bio (PPC-P96, New

23   York, USA). The PXB cells (96-well dish, 3×10^4 cells/well) were cultured in a specific

24   culture medium for PXB cells (Phoenix Bio) for one week before further analysis. KCs

1 (12-well dish, 1.5×10^5 cells/well) were purchased from ScienCell Research

2 Laboratories, Inc. (California, USA) and Lonza (Tokyo, Japan) and cultured in

3 Dulbecco's modified Eagle medium (DMEM, Wako, Osaka, Japan) supplemented with

4 10% fetal bovine serum and 1% penicillin–streptomycin (Thermo Fisher Scientific,

5 Kanagawa, Japan). These cells were incubated in a humidified atmosphere with 5% CO_2

6 at 37°C.

7

8 *Evaluation of M2BPGi levels in clinical serum samples*

9 The expression levels of M2BPGi in serum samples from the donor patients were

10 measured using a fully automated HSCL-2000i Immunoanalyzer (Sysmex Co., Hyogo,

11 Japan). The values of M2BPGi conjugated to WFA were indexed to the values

12 calculated as follows: cutoff index (C.O.I.) = ([M2BPGi] sample−[M2BPGi] negative

13 control)/([M2BPGi] positive control−[M2BPGi] negative control), where [M2BPGi]

14 sample represented the M2BPGi count of the serum sample (positive control; samples

15 with WFA treatment; NC, negative control). The positive control was supplied as a

16 calibration solution that was preliminarily standardized to yield C.O.I. = 1.0. [7]

17

18 *BrdU assay in PXB cells*

19 The conditioned medium (CM) of KCs with or without M2BPGi (3 ug/ml) was

20 collected 48 h later. The recombinant human M2BPGi was inherited from Sysmex

21 (Hyogo, Japan). For the BrdU assay to show the relation of M2BPGi-treated CM and

22 hepatocyte proliferation, the human hepatocyte PXB cells were cultured in DMEM

23 supplemented with 1% penicillin–streptomycin and the CM of KCs with or without

24 M2BPGi (3 ug/ml) in 12 h. According to the manufacturer's protocol, the cell

1   proliferation of the CM-cultured PXB cells was evaluated by the Cell Proliferation

2   enzyme-linked immunosorbent assay (ELISA) BrdU kit (Roche, Basel, Switzerland).

3

4   *Mass spectrometry*

5   To test the M2BPGi effect against KCs, KCs were cultured in DMEM supplemented

6   with 1% penicillin–streptomycin media with or without M2BPGi (3 ug/ml) for 48 h.

7   The culture media with or without M2BPGi were electrophoresed using sodium dodecyl

8   sulfate-polyacrylamide gel electrophoresis (SDS-PAGE) and then silver stained. The

9   proteins were extracted from each stained band obtained by the above experiment using

10   the in-gel digestion method. The digested bands are shown in Figure 1c as A, B, C, and

11   D. The protein identification of the digested bands was performed by ultrafleXtreme

12   (BRUKER, Massachusetts, USA).

13

14   *Western blotting*

15   Western blotting (WB) was performed as described previously,(13) using an antiGRP78

16   antibody (ab21685, 1:1,000 dilution; Abcam), ECL™ Prime WB Detection Reagent,

17   ImageQuant™ LAS 4000 imager (GE Healthcare, Buckinghamshire, UK), and ImageJ

18   software.

19

20   *BrdU assay in PXB cells with or without GRP78 treatment*

21   The GRP78 recombinant protein was purchased from MyBioSource (MBS718537, San

22   Diego, USA). For the BrdU assay to show the relation of GRP78 and hepatocyte

23   proliferation, the human hepatocyte PXB cells were cultured in the media with GRP78

24   (0, 400, 800, 1,600 ng/ml) for 12 h. According to the manufacturer's protocol, the

9

1   proliferation of the GRP78-treated PXB cells was evaluated by Cell Proliferation

2   ELISA BrdU kit (Roche, Basel, Switzerland).

3

4   *Cap analysis gene expression analysis*

5   The PXB cells (6 wells, 2.1×10^6 cells/well) were cultured in the media with or without

6   GRP78 (1,600 ng/ml) for 6 h. After a 6-h incubation, the cells were collected and

7   washed with phosphate-buffered saline (PBS), snap-frozen in nitrogen, and stored at

8   −80°C. The cap analysis gene expression (CAGE) library preparation, sequencing,

9   mapping, and gene expression and motif discovery analysis were performed by

10   DNAFORM (Kanagawa, Japan). Briefly, RNA quality was assessed using a

11   Bioanalyzer (Agilent) to ensure that the RNA integrity number exceeded 7.0 and the

12   A260/280 and A260/230 ratios exceeded 1.7. First-strand cDNAs were transcribed to

13   the 5′ ends of capped RNAs and attached to CAGE "bar code" tags. The sequenced

14   CAGE tags were then mapped to mouse (mm9) genomes using the BWA software

15   (v0.5.9) after discarding ribosomal or nonA/C/G/T base-containing RNAs. Finally, the

16   CAGE-tag 5′ coordinates were input for CAGEr clustering using the Paraclu algorithm

17   with the default parameters.[14]

18

19   *Surgical procedure of hepatectomy mouse models*

20   Seventy percent partial hepatectomy of mice was performed as described

21   previously.[15] We used 10-week-old male C57BL/6JJcl mice purchased from CLEA,

22   Japan. Animals were kept under a 12-h light-dark cycle. Mice were anesthetized using

23   isoflurane, and 70% hepatectomy was performed by resecting the liver's right and

24   middle lobes. After the operation, mice were placed in an incubator (37°C) for a brief

1   recovery period (10–15 min). Body weights were measured at the designated

2   postoperative endpoints (30 minutes, 1 hour, 3 hour, 6 hours, 1 day, 2 days, 3 days, 5

3   days, and 7 days after surgery) and blood samples were collected by cardiac puncture

4   under anesthesia with isoflurane. After that, the abdominal artery was cut for

5   euthanasia. Then, the liver was quickly removed and weighed and part of the liver tissue

6   was frozen in liquid nitrogen and stored at $-80°C$. The regenerated liver weight/body

7   weight ratios were calculated. Assuming that the liver weight removed at the time of

8   surgery is 70% of the total liver weight, the liver-regeneration rate was calculated from

9   the regenerated liver weight; (regeneration liver rate = regenerated liver weight/

10   predicted preoperative liver weight × 100, predicted preoperative liver weight =

11   resected liver weight [g]/0.7). The rest of the liver tissue was fixed in formalin to

12   prepare pathological slides. The size of hepatocytes was evaluated by counting the

13   number of cells per visual field at a magnification of 200× on POD1 when the swelling

14   of hepatocytes after hepatectomy is peaked.[16]

15   Ninety percent partial hepatectomy of mice was performed as described previously.[17]

16   The right lobe of the liver was resected in addition to the 70% hepatectomy, and only

17   the caudate lobe was preserved. A 50% glucose solution was intraperitoneally

18   administered at a volume of 1 ml/g body weight to prevent hypoglycemic attacks after

19   the operation. Many mice have died in the postoperative course of 90% hepatectomy;

20   thus, tissue and serum sampling were performed only 12 hours after surgery when the

21   mortality rate was still low. On the 15 mice, 90% hepatectomy, and sampling was

22   performed on the surviving mice 12 hours later (Survival rate: GRP78 (−): 6/15, 40%,

23   GRP78 (+): 11/15, 73.3%). The regenerated liver weight/body weight ratios were

24   calculated, and the liver-regeneration rate was calculated from the regenerated liver

11

1   weight (regeneration liver rate = regenerated liver weight/predicted preoperative liver

2   weight × 100, predicted preoperative liver weight = resected liver weight [g]/0.9). On

3   the 15 mice, 90% hepatectomy was performed and the survival rate was evaluated

4   separately from the mice sampled 12 hours later.

5   All experiments and procedures for care and treatment of mice in this study were

6   performed in accordance with the requirements of the Gunma University Animal Care

7   and Experimentation Committee (Experimental Protocol No.17-044).

8

9   ***Immunohistochemistry***

10   Resected mice liver specimens were fixed in 10% formaldehyde, embedded in paraffin

11   blocks, cut into 4-μm-thick sections, and mounted onto glass slides and staining using

12   standard immunohistochemistry methods.[18] Sections were incubated overnight at 4°C

13   with the following primary antibodies: antiGRP78 antibody (MBS9430977, 1:100

14   dilution; MyBioSource), antinitric oxide synthase (NOS) 2 antibody (ab3523, 1:50

15   dilution; Abcam), antiF4/80 antibody (ab111101, 1:50 dilution; Abcam), antismooth

16   muscle actin antibody (23081-1-AP, 1:200 dilution; proteintech, japan), antiM2BP

17   antibody (10281-1-AP,1:100 dilution; Proteintech, Japan), antiBrdU antibody (ab6326,

18   1:100 dilution; Abcam, Cambridge, UK), antiCyclinD1 antibody (ab16663, 1:100

19   dilution; Abcam) or antiCaspase3 antibody (ab184787, 1:100 dilution; Abcam).

20   Sections were washed in PBS and incubated with Histofine Simple Stain MAX-PO

21   (Nichirei Co., Tokyo, Japan) for 45 min at room temperature. Sections were then

22   counterstained with Mayer's hematoxylin solution and mounted. Negative controls were

23   incubated without the primary antibody, and no detectable staining was evident.

1 Quantitative evaluation of stained areas were analyzed using hybrid cell count

2 (Keyence, Osaka, Japan). [19]

3

4 *Immunofluorescence staining*

5 The sections were prepared, and endogenous peroxidase was blocked as described

6 above. The sections were then boiled in a citrate buffer (pH 6.4) for 10 min in a

7 microwave. Nonspecific binding sites were blocked by incubation with protein block

8 serum-free reagent for 30 min, and the sections were incubated with antiF4/80 antibody

9 (1:100 dilution), antiM2BP antibody (1:1,000 dilution), and antiα-SMA antibody (1:200

10 dilution) overnight at 4°C. Multiplex covalent labeling (F4/80; Cyanine 1, M2BP;

11 Cyanine 2, α-SMA; Cyanine 5) with amplification (TSA PLUS FLUORESCEIN,

12 NEL741001KT; PerkinElmer) was performed according to the manufacturer's protocol.

13 All sections were counterstained with 4',6-diamidino-2-phenylindole and examined

14 under an all-in-one BZ-X710 fluorescence microscope (Keyence).

15

16 *Evaluation of GRP78 levels in mouse serum by ELISA method*

17 Collected-mice blood samples were centrifuged at 5,000 rpm for 15 min at 4°C to

18 isolate the serum. After centrifugation, serum samples were stored at −80°C until the

19 ELISA analysis. GRP78 ELISA kits were purchased from MyBioSource and used

20 according to the manufacturer's protocol.

21

22 *KCs eradication by clodronate liposomes in the 70% hepatectomy mouse model*

23 Clodronate liposome (CL) (12.5 mg/kg mouse body weight) (CL, 16003631, Funakoshi,

24 Tokyo, Japan) was administered intraperitoneally to eradicate the KC function in the

13

1   70% hepatectomy mouse model 48 h before the liver resection. The hepatectomy

2   procedure, blood sampling, liver tissue collection, and the evaluation of GRP78 levels

3   in serum were performed as mentioned above.

4

5   *GRP78 administration in a hepatectomy mouse model*

6   In the GRP78 administration group (GRP78 [+] group), 100 ng/g body weight of

7   GRP78 recombinant protein (10 ng/ul PBS, MBS718537, MyBioSource) was

8   administered intraperitoneally immediately after 70% or 90% hepatectomy. In the

9   control group (GRP78 [−] group), 10 n/g body weight of PBS solution was administered

10   intraperitoneally at the same timing.

11

12   *BrdU assay in mice liver*

13   One-hundred milligram per kilogram BrdU (ab142567, Abcam) was intraperitoneally

14   injected 1 h before the remnant liver resection (POD1, POD2) in the mice undergoing

15   the 70% hepatectomy. Immunostaining of BrdU was performed as mentioned above.

16   The ratio of BrdU-positive cells per 1,000 hepatocyte cells was counted in three fields

17   per each tissue.

18

19   *Statistical analysis*

20   Data for continuous variables are expressed as means ± standard deviation (SD).

21   Differences among the multiple groups were evaluated by the analysis of variance

22   (ANOVA) test and Tukey's test. T-test was used to compare the two groups. Results

23   with P values of <0.05 were considered statistically significant. The Kaplan-Meier

1 estimator was used for survival-rate evaluation. The statistical software JMP 14.0.0

2 software package (SAS Institute Inc.) was used.

3

4 **Results**

5 *Relationship of postoperative serum M2BPGi and liver-regeneration rate*

6 The serum M2BPGi level in the donor of living donor liver transplant at three days after

7 the operation was positively correlated with the liver-regeneration rate evaluated by

8 postoperative CT scanning in 1 week after the operation (R = 0.598, P < 0.01; Figure

9 1a). The serum M2BPGi level was also positively correlated with the expected resected

10 liver volumes by before operation CT scanning (R = 0.620, P < 0.01; Figure 1a) and

11 actual resected liver weight (R = 0.680, P < 0.01; Figure 1a). This result indicated that

12 the resected liver volume affects the serum M2BPGi and liver-regeneration degree after

13 hepatectomy.

14

15 *Proliferation potency of human hepatocyte PXB cells by KCs CM with M2BPGi*

16 Mere M2BPGi administration into culture media did not affect the BrdU uptake by the

17 PXB cells. However, KC CM without M2BPGi increased the BrdU uptake of the cells

18 compared with the culture media group with or without M2BPGi (Figure 1b).

19 Interestingly, KC CM with M2BPGi increased the BrdU uptake of the PXB cells

20 compared with the other groups (P < 0.01) (Figure 1b).

21

22 *Identification of GRP78 as one of the extracted proteins in KCs treated with M2BPGi*

23 The M2BPGi-treated KCs could affect the status of CM because the KCs CM

24 significantly increased the proliferation potency of human hepatocytes (Figure 1b).

15

1 Therefore, we focused on the secretory proteins from KCs treated with M2BPGi. To

2 identify the unknown factors involved in hepatocyte proliferation, four expressing bands

3 were detected between KC CM with and without M2BPGi by SDS-PAGE and silver

4 staining methods (Figure 1c left panel). Using mass spectrometry, the A, B, C, and D

5 bands were identified as Mac-2 binding protein (M2BP), GRP78, albumin, and liver

6 carboxylesterase 1, respectively (Figure 1c right panel). The expression of GRP78 in

7 KCs CM with M2BPGi was higher than that of KCs CM without M2BPGi (Figure 1d).

8

9 *Effects of GRP78 on human hepatocytes*

10 The proliferation potency of PXB cells treated with GRP78 was evaluated by a BrdU

11 assay. The GRP78 administration into culture media increased the BrdU uptake of the

12 PXB cells compared with the culture media without GRP78 (Figure 2a). Differential

13 gene expression levels between PXB cells with and without GRP78 treatment were

14 evaluated by CAGE analysis. Gene ontology analysis clarified that cytokine-mediated

15 signaling pathway, inflammatory response, response to lipopolysaccharides, and

16 response to molecules of bacterial origin, including NOS2, were upregulated in PXB

17 cells with GRP78 compared with that without GRP78 (Supplementary Table 1).

18 Moreover, the expression of NOS2, DUOXA2, ZBED1, and the others in PXB cells

19 with GRP78 was higher than in those without GRP78 (Figure 2b).

20

21 *Induction pattern of GRP78 and M2BP in the regenerating liver after hepatectomy*

22 We evaluated the expression of GRP78, M2BP, KCs marker F4/80, and HSC marker α-

23 SMA in the remnant livers of the 70% hepatectomy mouse model. The expression of

24 M2BP, F4/80, α-SMA, and GRP78 was increased after the hepatectomy in the

1   sinusoidal area, and the expression was the strongest 12 h after the hepatectomy. The

2   expression of M2BP, α-SMA, and F4/80 was decreased to the preoperative level 24 h

3   after the hepatectomy. The expression of GRP78 24 h after hepatectomy was higher

4   than the preoperative level, but lower than 12h. (Figure 3a). The colocalization of KCs

5   marker F4/80 and M2BP was confirmed by immunofluorescence (IF). However, the

6   HSC cells with α-SMA were not expressing the M2BP protein (Figure 3b).

7

8   ***Induction of GRP78 in serum in a hepatectomy mouse model***

9   The serum levels of GRP78 were increased at the peak of 12 h after the hepatectomy

10   (Postoperative hours 0.5, 1, 3, 12, 24, 72, and 144; each N = 3) (Figure 4a upper panel).

11   Quantitative evaluation of GRP78 expression revealed peak expression at 12 hours,

12   consistent with the serum levels of GRP78 (Figure 4b lower panel). To investigate the

13   importance of KCs for serum GRP78 induction after hepatectomy, we established the

14   KCs eradication models by CL, a representative KCs inhibitor. The CL treatment

15   eradicated almost all KCs with F4/80 expression (Figure 4b lower panel). Moreover, the

16   serum levels of GRP78 12 h after hepatectomy in the CL administration group were

17   lower than that of the control group (Postoperative hour 12; each N = 5) (Figure 4b

18   upper panel).

19

20   ***Liver-regeneration-promoting effects of GRP78 in the 70% hepatectomy mouse model***

21   We compared the regenerative liver weight, regenerated liver/body weight ratio, and

22   liver-regeneration rate between 70% hepatectomy mice with or without GRP78

23   treatment (POD 1, 2, 3, 5, and 7; each N = 8). The postoperative regenerated liver

24   weight in the GRP78 administration group was higher than that of the control group at

1   POD2, 3, and 5 (Figure 5a left panel). The regenerated liver/body weight ratio in the

2   GRP78 administration group was higher than that of the control group at POD2, 3, and

3   5 (Figure 5a middle panel). The liver-regeneration rate in the GRP78 administration

4   group was higher than that of the control group at POD2, 3, 5, and 7 (Figure 5a right

5   panel). The number of postoperation BrdU-labeled hepatocytes was significantly

6   increased in the GRP78-administered group at POD1 and 2 (Figure 5b). Moreover, we

7   could validate the CAGE data of GRP78-treated human hepatocytes (Figure 2b),

8   indicating the NOS2 induction by GRP78 treatment in the regenerating liver of 70%

9   hepatectomy mouse model (Figure 5c). There was no significant difference between

10   groups treated with or without GRP78 in the number of hepatocytes in a visualized

11   field, which may express the volume of hepatocytes, suggesting that the hepatocyte

12   volume do not increase by administration of GRO78 after hepatectomy (Figure 5d, POD

13   1, N = 5).

14

15   ***KC eradication by CL significantly suppressed the GRP78-regulated liver***

16   ***regeneration in a hepatectomy mouse model***

17   The liver-regeneration rate in the CL administration group was lower than that of the

18   control group (Figure 6a left panel). The downregulation of the liver-regeneration rate

19   in the CL administration group was recovered in the CL/GRP78 combination group

20   (Figure 6a middle panel). The recovered liver-regeneration rate in the CL/GRP78

21   combination group was similar to that of the control group (Figure 6a right panel) (POD

22   1, 2, 3, 5, and 7, each N = 8), suggesting that GRP78 may cancel the CL-induced KCs

23   eradication effect that causes the suppression of liver regeneration in 70% hepatectomy

24   mouse models. Postoperation BrdU uptake was decreased in the CL administration

1   group. However, the downregulation of BrdU uptake by CL administration was

2   canceled in the CL/GRP78 combination group (Figure 6b).

3

4   ***Survival extension effect of GRP78 in the lethal 90% hepatectomy mouse model***

5   To examine the survival extension effect of GRP78, we established a lethal 90%

6   hepatectomy mouse model. Intraperitoneal administration of GRP78 after 90%

7   hepatectomy significantly improved the survival rate (each N = 15) (Figure 6c). Seven

8   mice were alive in a week after 90% hepatectomy in the GRP78 administration group,

9   whereas only one mouse in the control group survived. No significant difference was

10   observed in the postoperative regenerated liver weight between 90% hepatectomy mice

11   with or without GRP78 administration at 12 hours after hepatectomy. However, the

12   regenerated liver/body weight ratio and the liver-regeneration rate in the GRP78

13   administration group were higher than that of the control group at 12 hours after 90%

14   hepatectomy, although it is not an accurate evaluation because only the surviving mice

15   were examined (Figure 6d, GRP78(−): N = 6, GRP78(+): N = 11). Most mice treated

16   without GRP78 died within 7 days. Therefore, liver-regeneration rate of 90%

17   hepatectomy could not be evaluated at POD1–7. Serum LDH, ALT, and aspartate

18   aminotransferase (AST) levels 12 hours after 90% hepatectomy were significantly lower

19   in the GRP78 administration group (Supplementary Figure 1a, 90% hepatectomy,

20   GRP78(−): N = 6, GRP78(+): N = 11). No uptake was observed in any of the groups in

21   BrdU assay 12 hours after 90% hepatectomy. Therefore, we performed

22   immunohistochemistry using the Cyclin D1 antibody and evaluated the number of

23   Cyclin D1-positive cells. A significant increase in the Cyclin D1-positive rate was

24   observed in the GRP78-administered group (Supplementary Figure 1b). Additionally, a

19

1   significant decrease in the expression of Caspase 3 was observed in the GRP78-

2   administered group (Supplementary Figure 1c). Comparing the expression of F4/80

3   (marker of KCs), M2BP, and GRP78 between the 90% and 70% hepatectomy groups 12

4   hours after surgery, a significant increase in F4/80, M2BP, and GRP78 in the expression

5   was observed in the 90% group (Supplementary Figure 2a).

6

7   **Discussion**

8   M2BPGi promoted the production of GRP78 in KCs, and the KC-driven GRP78 had a

9   hepatocyte proliferation-promoting effect. The administration of GRP78 showed a liver-

10   regeneration-promoting effect in a murine model after 70% hepatectomy and increased

11   the survival rate after 90% hepatectomy. We propose that the M2BPGi secreted by

12   activated HSCs can facilitate the generation of KC-derived GRP78, which promotes

13   liver regeneration by activating the proliferation of hepatocytes (Figure 7).

14   We identified KC-secreted GRP78 as a new hepatotrophic factor that promotes

15   hepatocyte proliferation and liver-regeneration. GRP78 belongs to the HSP70 family

16   and acts as a molecular chaperone.[20] Moreover, we could clarify for the first time that

17   the GRP78 is a vital secretory factor for hepatocyte proliferation and liver regeneration

18   in the 70% hepatectomy mouse model and survival prolongation in a 90% hepatectomy

19   mouse model with lethal liver failure. GRP78 is mostly known as a marker for

20   endoplasmic reticulum (ER) stress and plays a role as a major ER chaperone with anti-

21   apoptotic properties, and liver damage in GRP78 liver-specific knockout mouse was

22   significantly increased under chronic hepatic disorders by alcohol, high fat diet, drugs,

23   and toxins via inhibition of hepatocyte ER homeostasis.[21] However, the recovery

24   effect of GRP78 administration against lethal liver failure after hepatectomy had not

1 been studied. From our data, the expression of Caspase3, which is the biomarker of

2 apoptosis, decreased in the GRP78-administered group after 90% hepatectomy. BrdU

3 was not uptook at 12 hours after hepatectomy, but the expression of Cyclin D1 was

4 upregulated in the GRP78-administered group after 90% hepatectomy. BrdU uptake

5 occurs in the synthesis (S) phase of the cell cycle, and the expression of Cyclin D1

6 occurs in the Gap 1 (G1) phase of the earlier cell cycle than S phase. Many hepatocytes

7 12 hours after 90% hepatectomy are in G1 phase, but hepatocytes of the GRP78-

8 administered group are more prepared for the transition to S phase.[22, 23]   From

9 these results, it is assumed that hepatocytes of the GRP78-administered group after 90%

10 hepatectomy are protected from apoptosis by the anti-apoptotic effect of GRP78 and

11 cell cycles of hepatocytes promoted at an early time. The survival prolongation and

12 regeneration-promoting effect after 90% hepatectomy by GRP78 are the anti-apoptotic

13 effects as the molecular chaperon. Our findings clearly suggest that the administration

14 of GRP78 may be one of the therapeutic tools to promote liver regeneration and protect

15 hepatocytes from apoptosis.

16 KCs are necessary for GRP78 secretion, as shown by the KC eradication experiments

17 using CL. GRP78 is a multifunctional protein that acts as a molecular chaperone in cells

18 of various organs.[24] In our experiment, almost all suppression of KCs did not

19 suppress all of serum GRP78, so that GRP78 production in cells other than KCs is also

20 suggested. Since suppression of KCs resulted in a 50% or more decrease in serum

21 GRP78, KCs are considered to be the main producer of serum GRP78 after

22 hepatectomy. The complex network between hepatocytes and parenchymal cells for live

23 regeneration consists of several secretory factors. Therefore, we thought that the system

24 of GRP78 secretion derived from activated KCs might be one of the important

21

1   component in the cellular networks. Until now, many researchers have reported GRP78

2   regulatory factors, such as cellular stress and several compounds.[24] Among them, our

3   group had already reported that M2BPGi treatment could activate the intracellular

4   signaling of the Mammalian target of rapamycin (mTOR).[8] Moreover, some

5   researchers reported that the activation of mTOR signaling induces the GRP78

6   expression in several cells.[25]   In this study, the colocalization of the KC marker

7   F4/80 and M2BP was confirmed by IF. In contrast, the HSCs with α-SMA did not

8   express the M2BP protein. This result is consistent with past results showing that

9   M2BPGi does not remain intracellularly in HSCs and that the secreted M2BPGi was

10   stained in KCs.(9) Therefore, the induction and secretion of GRP78 from KCs may be

11   regulated by the mTOR signaling of KCs through the external stimuli of M2BPGi.

12   We found that GRP78 induces NOS2 expression in hepatocytes. Hepatocytes, KCs, and

13   HSCs are prompted to express an intense NOS2 activity once exposed to effective

14   stimuli, such as bacterial lipopolysaccharide and cytokines.[26]   Nitric oxide (NO)

15   from NOS2 is released immediately after hepatectomy to become involved in liver

16   regeneration.[27] NOS2 is an important hepatoprotective factor in the regenerating liver

17   and has a crucial role in liver regeneration by protecting the remnant tissue from

18   apoptotic death.[28] In *Nos2*-knockout mice, liver regeneration after PH is delayed, and

19   there is an increase of the expression of genes related to apoptosis, such as Caspase3,

20   Caspase9, and *Bax*.[29] One of the hepatoprotective and antiapoptosis effects of GRP78

21   on the liver may be due to the regulation of NOS2 expression.

22   Mere administration of GRP78 may be a problem for patients with cancer after

23   hepatectomy because it has been reported that GRP78 is associated with tumor-

24   promoting effects in several cancers, including hepatocellular carcinoma (HCC),

1 similarly to the effects of secretory liver-regeneration factors such as hepatocyte growth

2 factor (HGF) and IL-6.[30, 31] HGF has been reported to primarily facilitate hepatocyte

3 survival and tissue remodeling at liver regeneration, and it has been promoted as a

4 potent therapeutic tool for liver failure.[32] However, HGF plays a crucial role not only

5 for liver regeneration in liver failure but also in the progression of HCC.[33] Similarly,

6 IL-6, which is important for liver regeneration, is involved in tumor progression and

7 drug resistance of HCC.[31] Moreover, it has been reported that GRP78 affects the

8 progression of HCC, cholangiocarcinoma, and colon cancer, which may cause the

9 metastatic liver tumor in the therapeutic time course.[34] Due to the potential of GRP78

10 for such cancers, we propose the use of GRP78 in donors of living liver

11 transplants, patients with liver failure after hepatectomy against noncancerous diseases,

12 and patients with fulminant hepatitis. Since GRP78 has an anti-apoptotic effect along

13 with the liver-regeneration proliferation effect, therapeutic effects for decompensated

14 cirrhosis are also expected. However, patients with decompensated cirrhosis usually

15 show high serum levels of M2BPGi.[6] Therefore, there is a possibility that the

16 M2BPGi/GRP78 axis is already activated and the therapeutic effect is expected to be

17 limited.

18

19 **Conclusion**

20 In this study, we demonstrated that the M2BPGi-activated KCs produce GRP78, which

21 facilitates liver regeneration via activation of the proliferation of hepatocytes. GRP78

22 administration immediately after 90% hepatectomy could improve the survival in a

23 lethal murine model. The new hepatotrophic factor GRP78 may be a promising

24 therapeutic tool for lethal liver failure.

23

1 **Acknowledgments**

2 We thank the staff at Bioresource Center, Gunma University Graduate School of

3 Medicine, and Sysmex Co. (Hyogo, Japan) for technical help. This work was carried out

4 in part at the Bioresource Center, Gunma University Graduate School of Medicine, and

5 Sysmex Co. (Hyogo, Japan).

6

7 **Disclosure Statement**

8 This study was supported by Grants-in-Aid for Scientific Research from the Japan

9 Society for the Promotion of Science; grant numbers: 19K09189.

10 Authors declare no Conflict of Interest for this article.

11

12 **References**

13 1.   Fausto N, Campbell JS, Riehle KJ. Liver regeneration. Hepatology.
14 2006;43:S45–53.
15 2.   Gilg S, Sandström P, Rizell M, Lindell G, Ardnor B, Strömberg C, et al. The
16 impact of post-hepatectomy liver failure on mortality: a population-based study. Scand J
17 Gastroenterol. 2018;53:1335–9.
18 3.   Ishikawa J, Takeo M, Iwadate A, Koya J, Kihira M, Oshima M, et al.
19 Mechanical homeostasis of liver sinusoid is involved in the initiation and termination of
20 liver regeneration. Commun Biol. 2021;4:409.
21 4.   Poisson J, Lemoinne S, Boulanger C, Durand F, Moreau R, Valla D, et al.
22 Liver sinusoidal endothelial cells: physiology and role in liver diseases. J Hepatol.
23 2017;66:212–27.
24 5.   Tsuchida T, Friedman SL. Mechanisms of hepatic stellate cell activation. Nat
25 Rev Gastroenterol Hepatol. 2017;14:397–411.
26 6.   Shirabe K, Bekki Y, Gantumur D, Araki K, Ishii N, Kuno A, et al. Mac-2
27 binding protein glycan isomer (M2BPGi) is a new serum biomarker for assessing liver
28 fibrosis: more than a biomarker of liver fibrosis. J Gastroenterol. 2018;53:819–26.
29 7.   Kuno A, Sato T, Shimazaki H, Unno S, Saitou K, Kiyohara K, et al.
30 Reconstruction of a robust glycodiagnostic agent supported by multiple lectin-assisted
31 glycan profiling. Proteomics Clin Appl. 2013;7:642–7.

8. Dolgormaa G, Harimoto N, Ishii N, Yamanaka T, Hagiwara K, Tsukagoshi M, et al. Mac-2-binding protein glycan isomer enhances the aggressiveness of hepatocellular carcinoma by activating mTOR signaling. Br J Cancer. 2020;123:1145–53.

9. Bekki Y, Yoshizumi T, Shimoda S, Itoh S, Harimoto N, Ikegami T, et al. Hepatic stellate cells secreting WFA(+) -M2BP: its role in biological interactions with Kupffer cells. J Gastroenterol Hepatol. 2017;32:1387–93.

10. Toshima T, Shirabe K, Ikegami T, Yoshizumi T, Kuno A, Togayachi A, et al. A novel serum marker, glycosylated Wisteria floribunda agglutinin-positive Mac-2 binding protein (WFA(+)-M2BP), for assessing liver fibrosis. J Gastroenterol. 2015;50:76–84.

11. Santamaria-Barria JA, Zeng S, Greer JB, Beckman MJ, Seifert AM, Cohen NA, et al. Csf1r or Mer inhibition delays liver regeneration via suppression of Kupffer cells. PLoS One. 2019;14:e0216275.

12. Zappa M, Dondero F, Sibert A, Vullierme MP, Belghiti J, Vilgrain V. Liver regeneration at day 7 after right hepatectomy: global and segmental volumetric analysis by using CT. Radiology. 2009;252:426–32.

13. Yamanaka T, Harimoto N, Yokobori T, Muranushi R, Hoshino K, Hagiwara K, et al. Nintedanib inhibits intrahepatic cholangiocarcinoma aggressiveness via suppression of cytokines extracted from activated cancer-associated fibroblasts. Br J Cancer. 2020;122:986–94.

14. Forrest AR, Kawaji H, Rehli M, Baillie JK, de Hoon MJ, Haberle V, et al. A promoter-level mammalian expression atlas. Nature. 2014;507:462–70.

15. Mitchell C, Willenbring H. A reproducible and well-tolerated method for 2/3 partial hepatectomy in mice. Nat Protoc. 2008;3:1167–70.

16. Miyaoka Y, Ebato K, Kato H, Arakawa S, Shimizu S, Miyajima A. Hypertrophy and unconventional cell division of hepatocytes underlie liver regeneration. Curr Biol. 2012;22:1166–75.

17. Hori T, Ohashi N, Chen F, Baine AM, Gardner LB, Hata T, et al. Simple and reproducible hepatectomy in the mouse using the clip technique. World J Gastroenterol. 2012;18:2767–74.

18. Tsunoda T, Inada H, Kalembeyi I, Imanaka-Yoshida K, Sakakibara M, Okada R, et al. Involvement of large tenascin-C splice variants in breast cancer progression. Am J Pathol. 2003;162:1857–67.

19. Miura Y, Ohkubo H, Niimi A, Kanazawa S. Suppression of epithelial abnormalities by nintedanib in induced-rheumatoid arthritis-associated interstitial lung disease mouse model. ERJ Open Res. 2021;7:00345-2021.

25

20. Radons J. The human HSP70 family of chaperones: where do we stand? Cell Stress Chaperones. 2016;21:379–404.

21. Ji C, Kaplowitz N, Lau MY, Kao E, Petrovic LM, Lee AS. Liver-specific loss of glucose-regulated protein 78 perturbs the unfolded protein response and exacerbates a spectrum of liver diseases in mice. Hepatology. 2011;54:229–39.

22. VanArsdale T, Boshoff C, Arndt KT, Abraham RT. Molecular pathways: targeting the cyclin D-CDK4/6 axis for cancer treatment. Clin Cancer Res. 2015;21:2905–10.

23. Inoue S. Analyses of cell cycle and DNA. Rinsho Byori (Jpn J Clin Pathol). 2001;49:835–41.

24. Bailly C, Waring MJ. Pharmacological effectors of GRP78 chaperone in cancers. Biochem Pharmacol. 2019;163:269–78.

25. Thon M, Hosoi T, Yoshii M, Ozawa K. Leptin induced GRP78 expression through the PI3K-mTOR pathway in neuronal cells. Sci Rep. 2014;4:7096.

26. Muriel P. Regulation of nitric oxide synthesis in the liver. J Appl Toxicol. 2000;20:189–95.

27. Carnovale CE, Scapini C, Alvarez ML, Favre C, Monti J, Carrillo MC. Nitric oxide release and enhancement of lipid peroxidation in regenerating rat liver. J Hepatol. 2000;32:798–804.

28. Zeini M, Hortelano S, Través PG, Gómez-Valadés AG, Pujol A, Perales JC, et al. Assessment of a dual regulatory role for NO in liver regeneration after partial hepatectomy: protection against apoptosis and retardation of hepatocyte proliferation. FASEB J. 2005;19:995–7.

29. Li D, Li J, Wang G, Qin Y, Niu Z, Li Z, et al. Delayed liver regeneration after partial hepatectomy in aged Nos2 knockout mice. Cell J. 2017;19:218–30.

30. Li R, Yanjiao G, Wubin H, Yue W, Jianhua H, Huachuan Z, et al. Secreted GRP78 activates EGFR-SRC-STAT3 signaling and confers the resistance to sorafeinib in HCC cells. Oncotarget. 2017;8:19354–64.

31. Bergmann J, Müller M, Baumann N, Reichert M, Heneweer C, Bolik J, et al. IL-6 trans-signaling is essential for the development of hepatocellular carcinoma in mice. Hepatology. 2017;65:89–103.

32. Huh CG, Factor VM, Sánchez A, Uchida K, Conner EA, Thorgeirsson SS. Hepatocyte growth factor/c-met signaling pathway is required for efficient liver regeneration and repair. Proc Natl Acad Sci U S A. 2004;101:4477–82.

33. Huang X, Gan G, Wang X, Xu T, Xie W. The HGF-MET axis coordinates liver cancer metabolism and autophagy for chemotherapeutic resistance. Autophagy. 2019;15:1258–79.

1 34.   Sharma SH, Rajamanickam V, Nagarajan S. Antiproliferative effect of p-
2 Coumaric acid targets UPR activation by downregulating Grp78 in colon cancer. Chem
3 Biol Interact. 2018;291:16–28.

4

5

6

7

8

9

10

11

12

13

14

15

16

17

18

19

20

21

22

23

24

25

27

1   **Figure Legends**

2   **Figure 1. Significance of M2BPGi on liver regeneration and M2BPGi-induced**

3   **GRP78 secretion by KCs.**

4   **a.** The serum M2BPGi level of the donor patients for living donor liver transplant three

5   days after the operations was correlated with the postoperative liver-regeneration rate at

6   1 week after the operations (R = 0.598   P < 0.001), expected resected liver volumes (R

7   = 0.620, P < 0.01), and actual resected liver weight (R = 0.680, P < 0.01).

8   **b**. BrdU assay of PXB cells (human hepatocyte) with or without M2BPGi (3 mg/ml)

9   and the PXB cells in KC CM with or without M2BPGi (3 mg/ml). KCs CM: Kupffer

10   cells' conditioned media, N = 8, ANOVA P < 0.01, *P < 0.01.

11   **c**. Mass spectrometry using the KC CM with or without M2BPGi. GRP78 as the B-band

12   was identified as one of the induced proteins in KC CM by M2BPGi treatment.

13   **d**. Confirmation of GRP78 induction in KC CM by M2BPGi treatment using WB.

14

15   **Figure 2. Effects of GRP78 on human hepatocytes (PXB cells).**

16   **a**. BrdU assay of PXB cells (human hepatocytes) with GRP78 (0, 400, 800, and 1,600

17   ng/ml). N = 8, ANOVA P < 0.01, *P < 0.05, **P < 0.01.

18   **b**. Differentially expressed genes in PXB cells treated with GRP78 using CAGE

19   analysis. These genes were selected as >6-fold change (GRP78 [+]/GPR78 [-]).

20

21   **Figure 3. Expression of GRP78 in serum and liver tissue after 70% hepatectomy in**

22   **mice.**

23   **a**. Immunohistochemical evaluation of M2BP, αSMA, F4/80, and GRP78 expression in

24   the liver after 70% hepatectomy. Magnification ×400. Scale bar indicates 50 μm.

1   **b**. Immunofluorescent evaluation of M2BP, F4/80, and αSMA in the liver 24 h after

2   70% hepatectomy. Magnification ×400.

3

4   **Figure 4. Expression of GRP78 in serum after 70% hepatectomy in mice.**

5   **a**. Upper panel: Serum GRP78 levels after 70% hepatectomy in mice increased at the

6   peak of 12 h after the hepatectomy. N = 3, ANOVA P < 0.01, *P < 0.05, **P < 0.01.

7   Lower panel: The positive cell area of GRP78 after 70% hepatectomy in mice increased

8   at the peak of 12 hours after the hepatectomy. N = 6, ANOVA P < 0.01, *P < 0.05, and

9   **P < 0.01.

10   **b**. Serum GRP78 levels after 70% hepatectomy in mice treated by clodronate liposome

11   (CL), as a representative KC inhibitor, at 12 h after the hepatectomy GRP78 levels were

12   decreased by CL treatment compared with the control group without CL. N = 5, *P <

13   0.05.

14

15   **Figure 5. Effects of GRP78 after 70% hepatectomy in mice.**

16   **a.** The left graph shows that GRP78 administration improved postoperative regenerated

17   liver weight (g) at 2–5 days after hepatectomy. N = 8. The middle graph shows that

18   GRP78 administration improved postoperative regenerated liver/body weight ratio (%)

19   2–5 days after hepatectomy. N = 8. The right graph shows that GRP78 administration

20   improved the liver-regeneration rate (%) two to seven days after hepatectomy. N = 8.

21   *P < 0.05, **P < 0.01.

22   **b**. Immunohistochemical evaluation of BrdU in the liver of 70% hepatectomy model

23   mice treated with or without GRP78. The liver samples were harvested at POD1 and

29

1   POD2 after hepatectomy. The right panel showed the BrdU-positive cell rate (%) in the

2   liver samples. N = 6. Magnification ×400. Scale bar indicates 50 μm.

3   **c**. Immunohistochemical evaluation of NOS2 expression in the liver of 70%

4   hepatectomy model mice treated with or without GRP78. The liver samples were

5   harvested at POD1 after hepatectomy. Magnification ×400. Scale bar indicates 50 μm.

6   **d**. The number of hepatocytes per visual field was N = 5. Magnification ×200. Scale bar

7   indicates 100 μm.

8

9   **Figure 6. Significance of KCs on GRP78-altered liver generation in the**

10   **hepatectomy mice model.**

11   **a**. Liver-regeneration rate (%) after 70% hepatectomy in mice treated with or without

12   CL and/or GRP78. The left panel shows the comparison between CL (−)/GRP78 (−)

13   and CL (+)/GRP78 (−), middle panel shows the comparison between CL (+)/GRP78 (+)

14   and CL (+)/GRP78 (−), and right panel shows the comparison between CL (−)/GRP78

15   (−) and CL (+)/GRP78 (+). N = 8. *P < 0.05, **P < 0.01.

16   **b**. Immunohistochemical evaluation of BrdU in the liver of 70% hepatectomy model

17   mice treated with or without CL and/or GRP78. The liver samples were harvested at

18   POD2 after hepatectomy. The upper panel shows the BrdU-positive cell rate (%) in the

19   liver samples. The lower panel shows the representative BrdU staining in each group.

20   N = 6. Magnification ×200. ANOVA P < 0.01, *P < 0.05, **P < 0.01. Scale bar

21   indicates 50 μm.

22   **c**. Survival curve of 90% hepatectomy mice model treated with GRP78 administration.

23   N = 15. P < 0.05.

1   **d**. The left graph shows that GRP78 administration improved postoperative regenerated

2   liver weight (g) at 12 hours after hepatectomy. The middle graph shows that GRP78

3   administration improved postoperative regenerated liver/body weight ratio (%) at 12

4   hours after hepatectomy. The right graph shows that GRP78 administration improved

5   the liver-regeneration rate (%) at 12 hours after hepatectomy. GRP78 (−): N = 6,

6   GRP78 (+): N = 11. *P < 0.05.

7

8   **Figure 7. The functional hypothesis of the M2BPGi/GRP78 axis in liver-**

9   **regenerating microenvironments.**

10   Activated HSCs after hepatectomy produce M2BPGi, which activates the KCs in the

11   liver, and then the activated KCs increase the concentration of GRP78 in the liver

12   microenvironments, which facilitates liver regeneration by activating the proliferation of

13   hepatocytes.

14

15   **Supplementary Figure 1. Effects of GRP78 after 90% hepatectomy in mice 12**

16   **hours after hepatectomy.**

17   **a**. Serum levels of LDH (IU/L), AST (IU/L), and ALT (IU/L), GRP78 (-): N = 6,

18   GRP78 (+): N = 11. *P < 0.05.

19   **b**. Immunohistochemical evaluation of BrdU and CyclinD1 in the livers of 90%

20   hepatectomy model mice treated with or without GRP78. The liver samples were

21   harvested at the 12th postoperative hour. The right panel showed the Cyclin D1-positive

22   cell rate (%) in the liver samples. N = 6. Magnification ×400. Scale bar indicates 50 μm.

23   **c**. Immunohistochemical evaluation of Caspase3 in the livers of 90% hepatectomy

24   model mice treated with or without GRP78. The liver samples were harvested at the 12th

31

1 postoperative hour. The right panel showed the Caspase3-positive cell area (%) in the

2 liver samples. *P < 0.01. N = 6. Magnification ×400. Scale bar indicates 50 μm.

3

4 **Supplementary Figure 2. Comparison of 70% hepatectomy model mice and 70%**

5 **hepatectomy model mice model**

6 **a**. Immunohistochemical evaluation of M2BP, F4/80, and GRP78 in the liver of 70%

7 hepatectomy model mice or 70% hepatectomy model mice model. The liver samples

8 were harvested at the 12th postoperative hour. The underpanel showed the positive cell

9 area (%) of M2BP, F4/80, or GRP78 in the liver samples. *P < 0.01. Magnification

10 ×400. Scale bar indicates 50 μm.
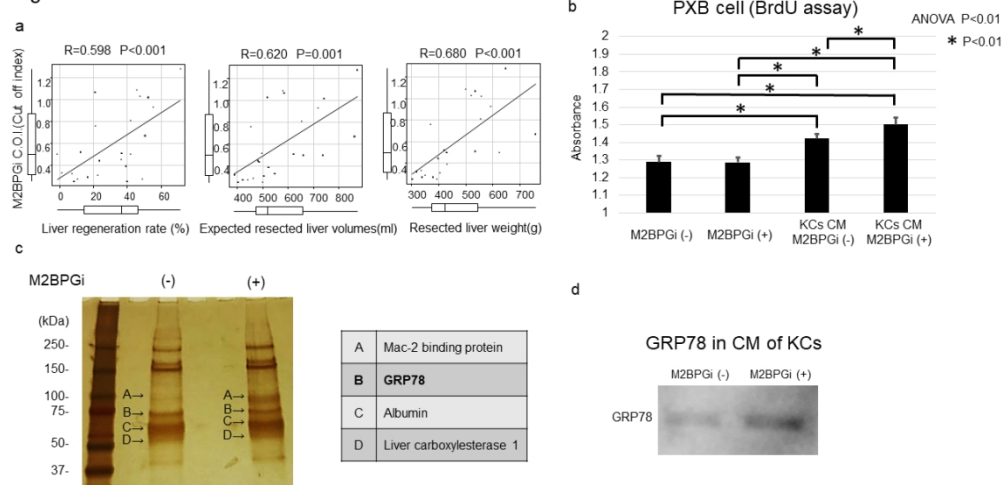
Figure 1. Significance of M2BPGi on liver regeneration and M2BPGi-induced GRP78 secretion by KCs.
a. The serum M2BPGi level of the donor patients for living donor liver transplant three days after the operations was correlated with the postoperative liver-regeneration rate at 1 week after the operations (R = 0.598   P < 0.001), expected resected liver volumes (R = 0.620, P < 0.01), and actual resected liver weight (R = 0.680, P < 0.01).
b. BrdU assay of PXB cells (human hepatocyte) with or without M2BPGi (3 mg/ml) and the PXB cells in KC CM with or without M2BPGi (3 mg/ml). KCs CM: Kupffer cells' conditioned media, N = 8, ANOVA P < 0.01, *P < 0.01.
c. Mass spectrometry using the KC CM with or without M2BPGi. GRP78 as the B-band was identified as one of the induced proteins in KC CM by M2BPGi treatment.
d. Confirmation of GRP78 induction in KC CM by M2BPGi treatment using WB.

338x190mm (96 x 96 DPI)

Figure 2
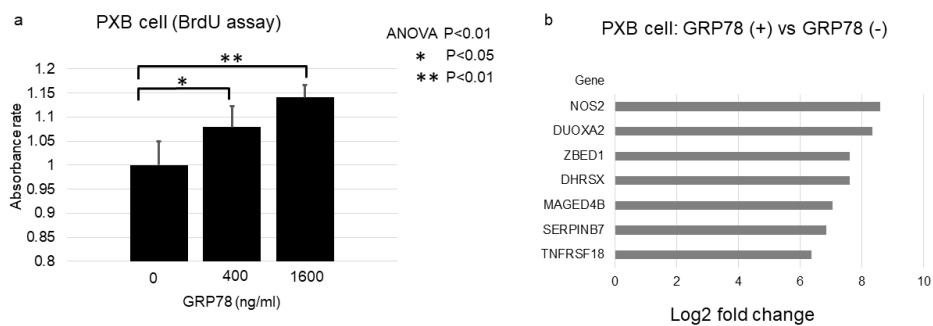
Figure 2. Effects of GRP78 on human hepatocytes (PXB cells).
a. BrdU assay of PXB cells (human hepatocytes) with GRP78 (0, 400, 800, and 1,600 ng/ml). N = 8, ANOVA
P < 0.01, *P < 0.05, **P < 0.01.
b. Differentially expressed genes in PXB cells treated with GRP78 using CAGE analysis. These genes were
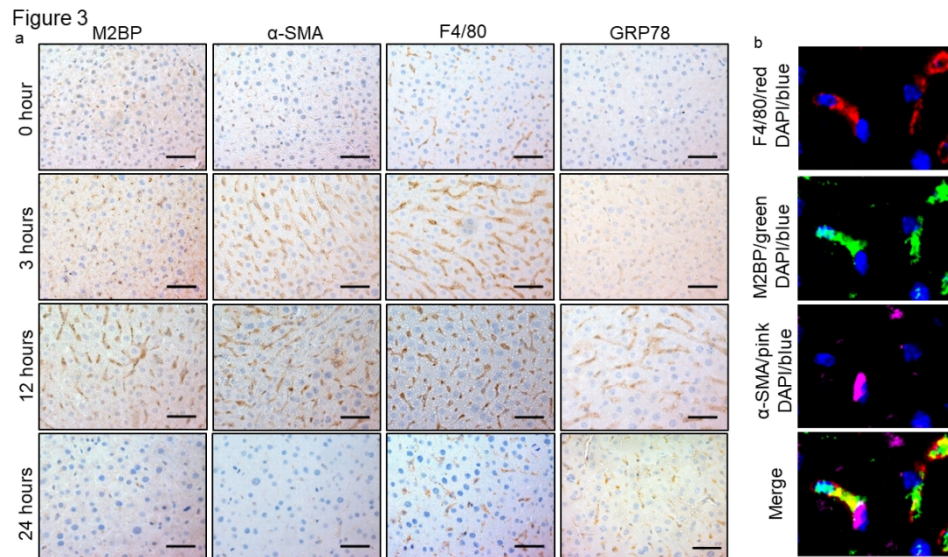selected as >6-fold change (GRP78 [+]/GPR78 [-]).

338x190mm (96 x 96 DPI)

Figure 3. Expression of GRP78 in serum and liver tissue after 70% hepatectomy in mice.
a. Immunohistochemical evaluation of M2BP, αSMA, F4/80, and GRP78 expression in the liver after 70% hepatectomy. Magnification ×400. Scale bar indicates 50 μm.
b. Immunofluorescent evaluation of M2BP, F4/80, and αSMA in the liver 24 h after 70% hepatectomy. Magnification ×400.

338x190mm (96 x 96 DPI)
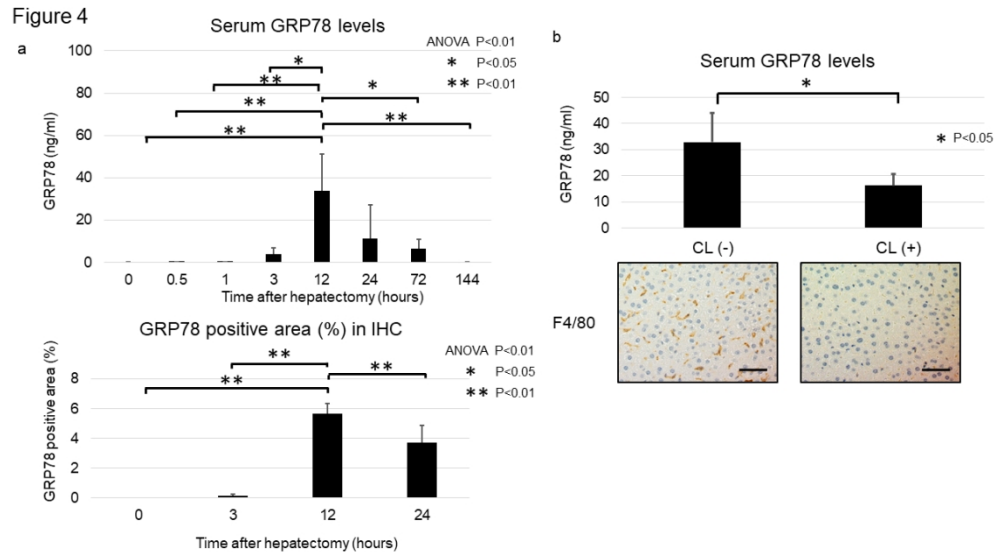
Figure 4. Expression of GRP78 in serum after 70% hepatectomy in mice.
a. Upper panel: Serum GRP78 levels after 70% hepatectomy in mice increased at the peak of 12 h after the hepatectomy. N = 3, ANOVA P < 0.01, *P < 0.05, **P < 0.01.
Lower panel: The positive cell area of GRP78 after 70% hepatectomy in mice increased at the peak of 12 hours after the hepatectomy. N = 6, ANOVA P < 0.01, *P < 0.05, and **P < 0.01.
b. Serum GRP78 levels after 70% hepatectomy in mice treated by clodronate liposome (CL), as a representative KC inhibitor, at 12 h after the hepatectomy GRP78 levels were decreased by CL treatment compared with the control group without CL. N = 5, *P < 0.05.

338x190mm (96 x 96 DPI)
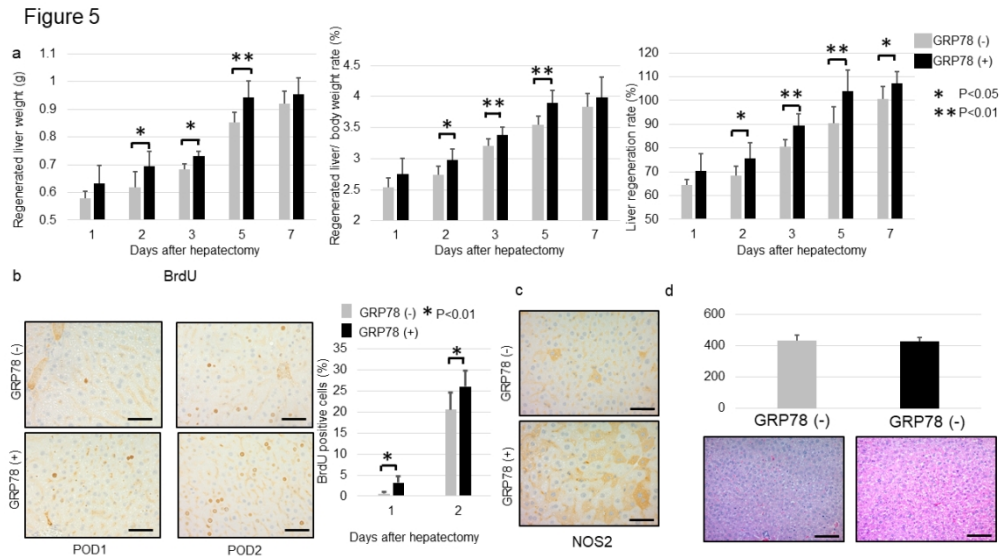
Figure 5

Figure 5. Effects of GRP78 after 70% hepatectomy in mice.
a. The left graph shows that GRP78 administration improved postoperative regenerated liver weight (g) at 2–5 days after hepatectomy. N = 8. The middle graph shows that GRP78 administration improved postoperative regenerated liver/body weight ratio (%) 2–5 days after hepatectomy. N = 8. The right graph shows that GRP78 administration improved the liver-regeneration rate (%) two to seven days after hepatectomy. N = 8. *P < 0.05, **P < 0.01.
b. Immunohistochemical evaluation of BrdU in the liver of 70% hepatectomy model mice treated with or without GRP78. The liver samples were harvested at POD1 and POD2 after hepatectomy. The right panel showed the BrdU-positive cell rate (%) in the liver samples. N = 6. Magnification ×400. Scale bar indicates 50 μm.
c. Immunohistochemical evaluation of NOS2 expression in the liver of 70% hepatectomy model mice treated with or without GRP78. The liver samples were harvested at POD1 after hepatectomy. Magnification ×400. Scale bar indicates 50 μm.
d. The number of hepatocytes per visual field was N = 5. Magnification ×200. Scale bar indicates 100 μm.
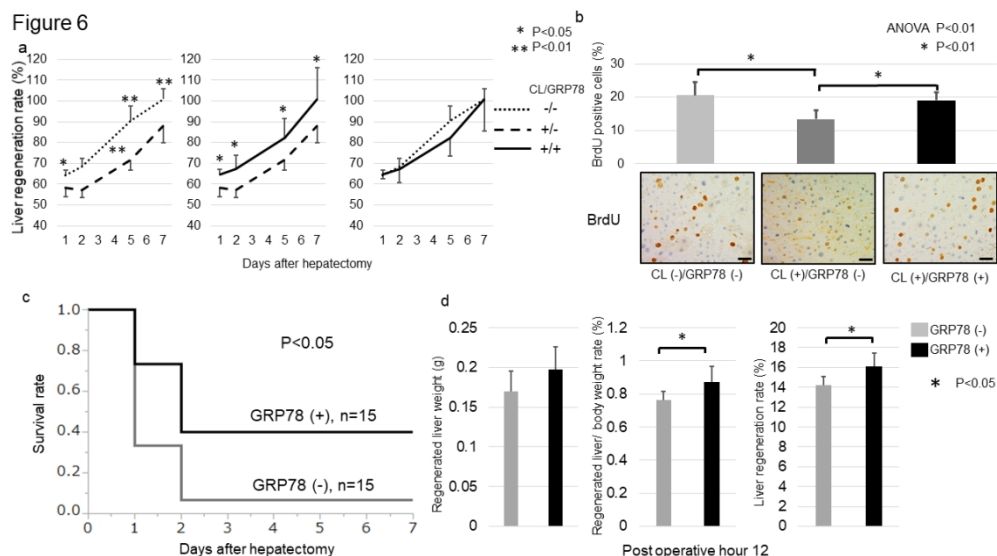

338x190mm (96 x 96 DPI)

Figure 6. Significance of KCs on GRP78-altered liver generation in the hepatectomy mice model.
a. Liver-regeneration rate (%) after 70% hepatectomy in mice treated with or without CL and/or GRP78. The left panel shows the comparison between CL (−)/GRP78 (−) and CL (+)/GRP78 (−), middle panel shows the comparison between CL (+)/GRP78 (+) and CL (+)/GRP78 (−), and right panel shows the comparison between CL (−)/GRP78 (−) and CL (+)/GRP78 (+). N = 8. *P < 0.05, **P < 0.01.
b. Immunohistochemical evaluation of BrdU in the liver of 70% hepatectomy model mice treated with or without CL and/or GRP78. The liver samples were harvested at POD2 after hepatectomy. The upper panel shows the BrdU-positive cell rate (%) in the liver samples. The lower panel shows the representative BrdU staining in each group. N = 6. Magnification ×200. ANOVA P < 0.01, *P < 0.05, **P < 0.01. Scale bar indicates 50 µm.
c. Survival curve of 90% hepatectomy mice model treated with GRP78 administration. N = 15. P < 0.05.
d. The left graph shows that GRP78 administration improved postoperative regenerated liver weight (g) at 12 hours after hepatectomy. The middle graph shows that GRP78 administration improved postoperative regenerated liver/body weight ratio (%) at 12 hours after hepatectomy. The right graph shows that GRP78 administration improved the liver-regeneration rate (%) at 12 hours after hepatectomy. GRP78 (−): N = 6, GRP78 (+): N = 11. *P < 0.05.
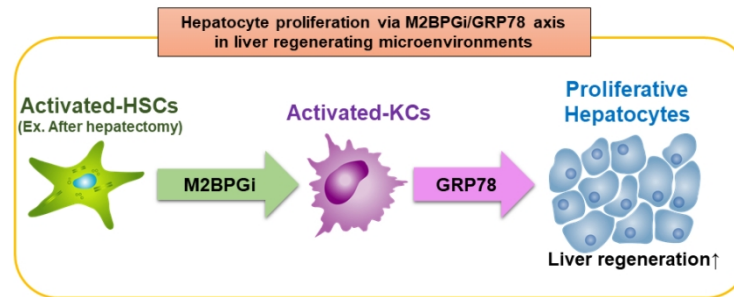
338x190mm (96 x 96 DPI)

Figure 7

Figure 7. The functional hypothesis of the M2BPGi/GRP78 axis in liver-regenerating microenvironments. Activated HSCs after hepatectomy produce M2BPGi, which activates the KCs in the liver, and then the activated KCs increase the concentration of GRP78 in the liver microenvironments, which facilitates liver regeneration by activating the proliferation of hepatocytes.

338x190mm (96 x 96 DPI)
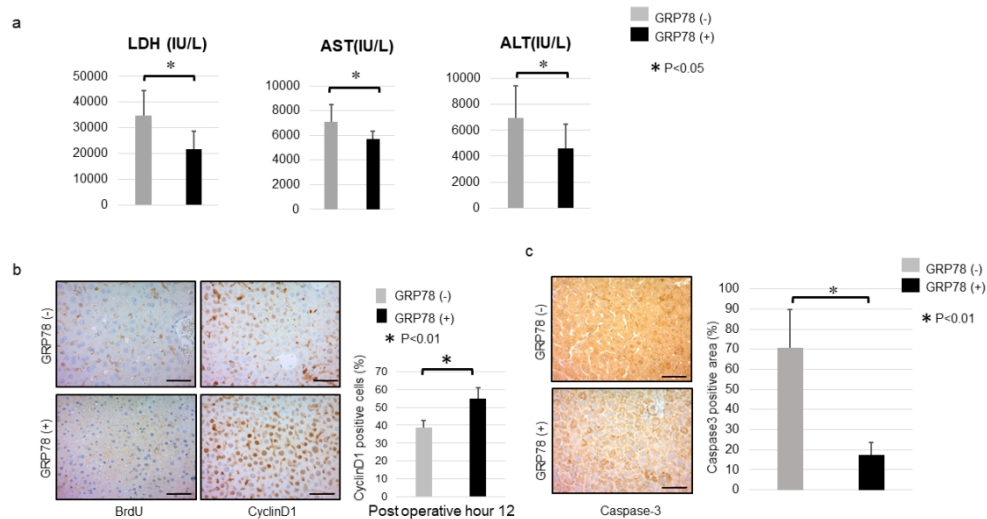
Supplementary Figure 1. Effects of GRP78 after 90% hepatectomy in mice 12 hours after hepatectomy.
a. Serum levels of LDH (IU/L), AST (IU/L), and ALT (IU/L), GRP78 (-): N = 6, GRP78 (+): N = 11. *P < 0.05.
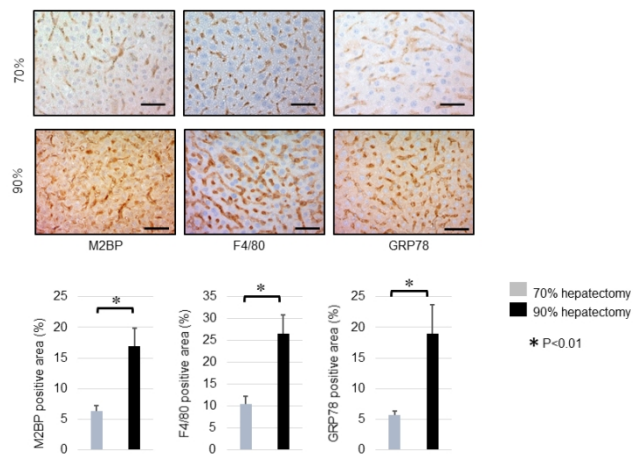b. Immunohistochemical evaluation of BrdU and CyclinD1 in the livers of 90% hepatectomy model mice treated with or without GRP78. The liver samples were harvested at the 12th postoperative hour. The right panel showed the Cyclin D1-positive cell rate (%) in the liver samples. N = 6. Magnification ×400. Scale bar indicates 50 μm.
c. Immunohistochemical evaluation of Caspase3 in the livers of 90% hepatectomy model mice treated with or without GRP78. The liver samples were harvested at the 12th postoperative hour. The right panel showed the Caspase3-positive cell area (%) in the liver samples. *P < 0.01. N = 6. Magnification ×400. Scale bar indicates 50 μm.

338x190mm (96 x 96 DPI)

Supplementary Figure2.

a

Supplementary Figure 2. Comparison of 70% hepatectomy model mice and 70% hepatectomy model mice model

a. Immunohistochemical evaluation of M2BP, F4/80, and GRP78 in the liver of 70% hepatectomy model mice or 70% hepatectomy model mice model. The liver samples were harvested at the 12th postoperative hour. The underpanel showed the positive cell area (%) of M2BP, F4/80, or GRP78 in the liver samples. *P < 0.01. Magnification ×400. Scale bar indicates 50 μm.

338x190mm (96 x 96 DPI)

SupplementaryTable1. Gene ontology analysis of PXB cells after treatment of GRP78

Gene Ontology	Gene Ratio	P value	Gene ID
Cytokine-mediated signaling pathway	12/23	7.20E-11	**NOS2**/TNFRSF9/CSF3/CCL7/CCL2/CXCL6/IL1RN/DUOX2/VCAM1/CXCL3/CXCL1/TNFRSF18
Inflammatory response	11/23	9.22E-11	**NOS2**/TNFRSF9/CCL7/CCL2/CXCL6/IL1RN/DUOXA2/VCAM1/CXCL3/CXCL1/TNFRSF18
Response to lipopolysaccharide	9/23	2.17E-10	**NOS2**/TNFRSF9/CSF3/CCL2/CXCL6/VCAM1/CXCL3/CXCL1/TNFRSF18
Response to molecule of bacterial origin	9/23	3.28E-10	**NOS2**/TNFRSF9/CSF3/CCL2/CXCL6/VCAM1/CXCL3/CXCL1/TNFRSF18
Neutrophil chemotaxis	5/23	1.02E-08	CCL7/CCL2/CXCL6/CXCL3/CXCL1
Regulation of leukocyte migration	6/23	1.75E-08	CCL7/CCL2/CXCL6/CXCL3/CXCL1/TNFRSF18
Neutrophil migration	5/23	1.86E-08	CCL7/CCL2/CXCL6/CXCL3/CXCL1
Regulation of signaling receptor activity	7/23	7.48E-08	CSF3/CCL7/CCL2/CXCL6/IL1RN/CXCL3/CXCL1
Regulation of chemotaxis	5/23	1.82E-06	CCL7/CCL2/CXCL6/CXCL3/CXCL1

* Gene expression ratio of GRP78 (+)/GRP78 (-) >4.

338x190mm (96 x 96 DPI)